Anisotropic optical properties of arrays of gold nanorods embedded in alumina

Ron Atkinson, William R. Hendren, Gregory A. Wurtz, Wayne Dickson, Anatoly V. Zayats, Paul Evans, and Robert J. Pollard
Centre for Nanostructured Media, School of Mathematics and Physics, The Queen's University of Belfast, University Road,
Belfast, BT7 1NN, United Kingdom
(Received 7 February 2006; published 5 June 2006)

A series of thin films comprising gold nanorods embedded in an alumina matrix have been fabricated with lengths ranging from 75 to 330 nm. Their optical properties, expressed in terms of extinction $-\ln(T)$, where T is optical transmittance, have been measured as a function of wavelength, rod length, angle of incidence, and incident polarization state. The results are compared to a Maxwell-Garnett based theory modified to take into account the strongly anisotropic nature of the medium. Transverse and longitudinal plasmon resonances are observed. The interaction between the nanorods leads to the splitting of the longitudinal resonance with the longer-wavelength resonance being forbidden for direct optical observations. The shorter-wavelength resonance related to the symmetric coupling between longitudinal plasma excitations in the nanorods depends on rod length, polarization state, and angle of incidence of the probing light. The impact of electron confinement on the optical properties of the gold rods is also seen and may be incorporated into the Maxwell-Garnett theory by restricting the mean free path of the conduction electrons to produce excellent agreement between observations and the complete theory. Annealing experiments that modify the physical structure of the gold confirm this conclusion.

INTRODUCTION

From the early 1990s, there has been increasing interest in the optical properties of nanoscale composite media where variously shaped metallic particles are embedded in a dielectric host medium. These metallic particles may be nonmagnetic, as has been the case for several studies of the noble metals Au, Ag, and Cu [1–3] or they may be magnetic, such as when the transition metal elements Fe, Ni, and Co [4,5] are used. The latter gives rise to magneto-optic interactions that have interesting properties in their own right.

The study of the optical properties of nanoparticles embedded in a dielectric matrix is by no means new and much work was done in the 1970s on media, then referred to as cermets, [6,7] where arrays of metallic/magnetic particles were produced in an insulating matrix by vacuum deposition techniques. More recently, there has been a revival of interest in the subject owing to the discovery that regular arrays of cylindrical pores can be produced by the electrolysis of aluminum thin films into alumina, and that these can subsequently be filled with another medium. This technique has been used to form a near-hexagonal array of metallic rods of controllable diameter and length embedded within an alumina matrix. By removing the alumina, it is even possible to fabricate an array of freestanding rods in air, though, of course, sitting on some substrate medium.

The optical properties of these structures are of considerable interest for several reasons. First, in their current primitive form they are highly anisotropic, with the degree of anisotropy being controlled by the rod dimensions and spacing. Second, the dimensions can be, and usually are, in a regime where their theoretical consideration can become extremely tedious and therefore stand as a testing ground against the most rigorous analysis. Third, the potential for new material properties, not seen in nature, such as negative refractive index[8] and negative permeability,[9,10] is tantalizing.

In this paper we report the results of a comprehensive set of measurements of the optical properties of a series of gold rod arrays embedded in an alumina matrix. Specifically, we present measurements of optical extinction $[-\ln(T)$, where T is optical intensity transmittance], for radiation polarized with its electric field vector perpendicular to the rod axis (S-state) or having a component parallel to it (P-state). This is done for the wavelength range 350–900 nm and for angles of incidence ranging from 0° to 60°.

To deal with the measurable optical properties of nanorods it is necessary to adopt some theoretical model for their description. Many theories have been developed in the past that attempt to describe the optical responses of nanoparticles. For example Mie[11] and Gans[12] solved Maxwell's equations explicitly for spheres and spheroids, and various authors have made use of these and similar formulations to explain the qualitative features of their observations. Others have made use of an effective medium approach such as the Maxwell-Garnett (MG) theory.[13]

In order to interpret our observations we apply the Maxwell-Garnett theory modified to take into consideration the anisotropic nature of the medium and derive the permittivity tensor that in this case applies to a uniaxial material where the optic axis is perpendicular to the plane of the substrate on which the rods sit. In addition, and to explain the details of the observations, we explore the effect that electron confinement has on the optical properties of the gold rods and hence on the collective optical properties of the arrays.

FABRICATION PROCEDURE

Aluminum films were grown on buffer layers of gold and tantalum pentoxide on glass substrates by dc magnetron sputter deposition (Fig. 1). Anodization and hence pore formation, was carried out at constant voltage using a platinum
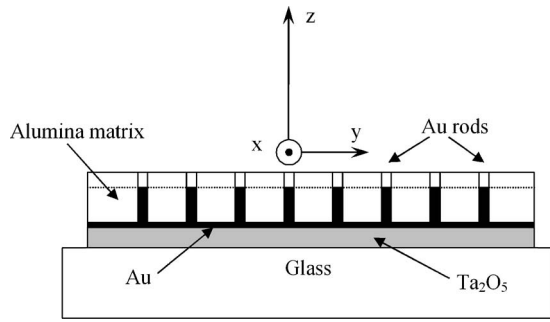
FIG. 1. Schematic of the idealized structure of the gold nanorods embedded in an alumina matrix.

counter-electrode. The electrolyte was cooled and the temperature monitored throughout the process. The pore template was then filled with gold, thus forming an array of nanorods. The tantalum oxide was necessary as an adhesion layer to avoid delamination on anodization of the aluminum and was also chosen because of its high transmittance in the visible spectrum.

The size and spacing of the pores is found to be linearly dependent on the anodisation voltage.[14] For this work the aluminum was anodized at 20 V in 0.3 M sulphuric acid which produced 20 nm diameter pores with ~40 nm spacing, giving an estimated number density of 4.8×10^{-4} pores/rods per $(nm)^2$ area of substrate. Gold rods were grown by direct electrodeposition from a non-cyanide gold plating solution.[15] The length of the rods was varied by changing the deposition time.

STRUCTURAL CHARACTERIZATION OF NANORODS

For the purposes of optical modeling, the thin-film structure is idealized to that shown in Fig. 1. This consists of a four-layer system. The top layer is an alumina layer with air-filled, rod-shaped holes followed by the important layer, where the alumina is charged with the Au rods. Below this are continuous layers of Au and Ta_2O_5 of thicknesses 5 and 9 nm, respectively. The actual structures are revealed by electron microscopy and shown in Fig. 2, in cross section (a) for 330 nm rods, and in plan view (b) showing the arrays of rods. The unfilled holes are seen above the gold rods and the buffer layers can be seen below the rods followed by the glass substrate. It is not possible to distinguish between the Au and Ta_2O_5 layers in the image.

THEORY

For the general case, the calculation of the optical properties of an array of particles is complicated. This is particularly so when the dimensions of the particle are comparable with the wavelength of the radiation or where the distance between the particles is small or where the particle distribution in space is either nonordered or nonrandom, and two-dimensional rather than three-dimensional. In the extreme case, the most rigorous analysis would treat the problem as an interacting assembly of atoms of known polarizability being driven by an incoming plane wave and all other waves
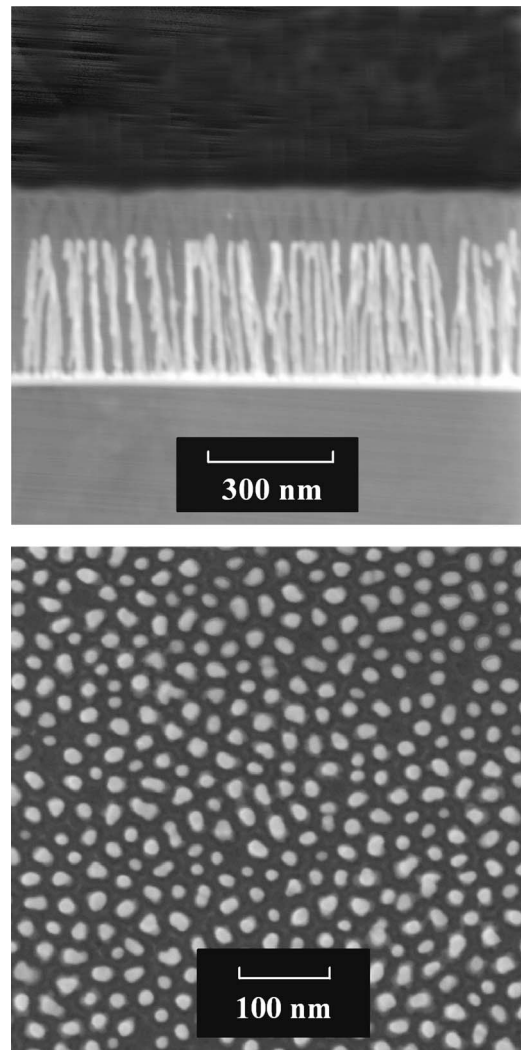
FIG. 2. Electron micrograph of (a) the cross section of a sample where the gold rod layer is ~330 nm thick. The top alumina layer is ~99 nm thick and the substrate is glass. (b) Plan view of 200 nm long gold rods grown in ~20 nm diameter pores. It is estimated that the number of pores filled is very close to 100%.

whose sources are all other atoms in the system.[16] Once the dipole moment of each and every atom is known the reflected and transmitted waves can be computed. Such calculations are simple in principle, but in practice are very demanding on computer resources. Moreover, the polarization of atoms in a particle is unlikely to be the same as for atoms in the bulk form of the material. Consequently, it is useful in the first instance to adopt a simple model that can be used quickly and efficiently to explore the behavior of the system and to compare its predictions with observations. As long as any assumptions, simplifications, and limitations are borne in mind, this is an acceptable way to proceed initially.

Since previous authors[17,18] have reported its success with regard to understanding the optical properties of nanorods we adopt the well known Maxwell-Garnett approach. However, we must generalize the theory to the case of an optically anisotropic system. In this case it is relatively simple to show that the generalized Maxwell-Garnett expression written in its tensor form, is

$$([K_c] - K_d[I])([K_c] - K_d[[I] - [\gamma]^{-1}])^{-1}$$
$$= f\{K_m[L] + K_d([I] - [L])\}^{-1}(K_m[I] - K_d[I])[\gamma], \quad (1)$$

where K_d and K_m are the isotropic dielectric constants of the host medium (alumina) and the metal rods (gold), respectively; $[K_c]$ is the dielectric tensor describing the optical properties of the nanorod array where the volume fraction of rod material in the host is $f(=\pi b^2 N/4)$; N is the number of rods per unit area of the substrate; b is the rod diameter; and $[I]$ is the unit tensor. The tensors $[K_c]$, $[\gamma]$, and $[L]$ are given by

$$[K_c] = \begin{bmatrix} K_x & 0 & 0 \\ 0 & K_x & 0 \\ 0 & 0 & K_z \end{bmatrix}, \quad (2)$$

$$[\gamma] = \begin{bmatrix} \gamma_x & 0 & 0 \\ 0 & \gamma_x & 0 \\ 0 & 0 & \gamma_z \end{bmatrix}, \quad (3)$$

and

$$[L] = \begin{bmatrix} L_x & 0 & 0 \\ 0 & L_x & 0 \\ 0 & 0 & L_z \end{bmatrix}, \quad (4)$$

where the z axis is perpendicular to the film plane, as shown in Fig. 1, and the tensor $[K_c]$ has its uniaxial form. Strictly, $[\gamma]$ is the tensor describing the interactions between the particles of the system that in the simplest case corresponds to the Lorentz local field $\underline{P}_m/3\epsilon_0$ where $\underline{P}_m$ is the polarization of the particles. In the simple case, therefore, $\gamma_x = \gamma_z = 1/3$. However, here the particle distribution is not three-dimensional, rather they form a two-dimensional interacting array and we might ultimately expect $\gamma_x \neq \gamma_z$. For this work, and because the particle dimensions and spacing make an absolute determination of $[\gamma]$ nontrivial, we will assume that $[\gamma] = (1/3)[I]$, following previous authors,[17,18] though it is convenient to allow for some deviation from this condition.

$[L]$ is the depolarization tensor that takes into account the shape of the particle and determines its polarizability through the intrinsic permittivity of the material from which it is composed. In this case, we have long rods that are assumed to approximate to prolate spheroids. Where the particle dimensions are assumed small compared to the wavelength of the radiation and the rod length is a and its diameter b,

$$L_z = \frac{1 - e^2}{e^2}\left[\frac{1}{2e}\ln\left(\frac{1+e}{1-e}\right) - 1 \right] \quad (5)$$

and

$$L_x = \frac{1 - L_z}{2}, \quad (6)$$

where $e^2 = (1 - b^2/a^2)$ and $b/a < 1$ is the particle aspect ratio.[19] If the rod length becomes less than its diameter, we assume the particles are just nucleated and are best approximated as spheres, in which case $L_x = L_z = 1/3$.

It follows that the two principal effective refractive indices $n_x = \sqrt{K_x}$ and $n_z = \sqrt{K_z}$ of a nanocomposite material may be obtained from Eq. (1) and can be expressed as

$$K_\sigma = K_d\left(1 + \frac{f\alpha_\sigma}{1 - f\alpha_\sigma\gamma_\sigma} \right), \quad (7)$$

where the subscript $\sigma(=x,z)$ refers to the principal directions and

$$\alpha_\sigma = \frac{K_m - K_d}{L_\sigma(K_m - K_d) + K_d},$$

is the polarizability per unit volume of the rods.

The principal refractive indices determine the optical properties of the nanorod array that is now treated as a thin, homogeneous, anisotropic layer. For S-polarized radiation where the electric field is always perpendicular to the axis of the rods, the effective refractive index n_S is simply equal to n_x. In contrast, for radiation polarized in the P-plane, the refractive index n_P involves components of both n_x and n_z, and for an angle of incidence ϕ_0 in air is given by[20]

$$n_P = \sqrt{n_x^2 + n_0^2 \sin(\phi_0)^2\left[1 - \frac{n_x^2}{n_z^2} \right]}. \quad (8)$$

The procedure for calculating the intensity transmittance, reflectance and absorptance then follows the usual methods which can be conveniently performed using 4×4 or 2×2 matrix methods or by using the well known reiterative formulations.[21] It is emphasized that the output from such calculations are absolute and may be compared directly to experimental data in a quantitative manner without the need for arbitrary units.

Before proceeding, the limitations of these formulations must be emphasised. First, the Maxwell-Garnett theory strictly only applies when the particle size and spacing is small (dilute system) when compared to the wavelength of the radiation. Second, the dipole-dipole interaction we shall assume is simple and close to the Lorentz value, as pointed out above. Despite these restrictions, past reports[17,18] have shown the model to be reasonable and, as we shall demonstrate here, it does provide a surprisingly good description of many of the details of the observations. It is stressed that improvements are possible in principle, as outlined earlier, by taking into account retardation effects for the many interacting dipoles.[22,23] However, this is not a simple procedure when measurements on multilayered structures are being considered in a quantitative manner.

RESULTS

For the optical multilayer system we are considering (Fig. 1), the upper layer is an alumina film with cylindrical rods of air. The above formulations may be applied to this layer, but for all practical purposes it can be treated as being isotropic with a refractive index slightly less than that of Al_2O_3 and quite close to that of common glass ($n_g \approx 1.51$). Below this layer is the film incorporating the metallic nanorods, whose thickness is set equal to that of the rod length. The rod

lengths were determined by electron microscopy to be 75, 165, and 330±10 nm. Likewise, the corresponding alumina/air-rod layer thicknesses were, 233, 187, and 99±10 nm, respectively. Below the rod layer are two buffer layers: a 5 nm gold layer and a 9±1 nm Ta_2O_5 layer. These were determined by x-ray diffraction and/or ellipsometry.

Using a bare glass substrate as a reference, measurements of optical transmittance (T) were made over the spectral range 350–950 nm at angles of incidence from 0° to 60° for both incident S- and P-polarized radiation, without polarization analysis of the transmitted light. Following previous work and therefore to conveniently compare our results with the data of others, we express the transmittance data as extinction, as defined above. It should be emphasised that optical extinction which is a measure of $-\ln(1-A-R-S)$, where A is absorptance and R is intensity reflectance, includes losses related to both absorption, reflection, and nonspecular scattering (S) in the film. Hence, peaks in extinction spectra cannot simply be referred to as absorption peaks, since one cannot always disregard the effect of reflection losses, which can be quite high in thin-film systems.

The results are shown in Figs. 3(a)–3(c), and the most important features of these curves are as follows. In all cases the curves indicate a peak (*green peak*) in the extinction spectra at a wavelength of about 525 nm, which is assigned to the excitation of the dipolar transverse plasmon resonance associated with radiation polarized with its *E*-vector perpendicular to the axis of the rod. Although expectations based on theoretical calculations using optical data for bulk gold indicate that the position of this peak should undergo a small blueshift with increasing rod aspect ratio, this is difficult to observe in the experiments owing to significant width of this peak. A second, much stronger (*red peak*) occurs at longer wavelengths (~700 nm for this layer geometry), which only appears when radiation is polarized in the P-state. The magnitude of the red peak is strongly dependent on the angle of incidence, as it increases with increasing projection of the incident electric field along the rods. The resonance position of the red peak has also been observed, to be slightly angular dependent with the peak shifting to a shorter wavelength with the increase of the angle of incidence of the probe light. This is only slightly visible in Fig. 3(b) and we illustrate this trend later in an annealed sample. For a given volume fraction, determined by rod diameter and spacing, the red peak position is strongly sensitive to the rod length. As the rod length decreases, the peak is reduced and shifts towards shorter wavelengths until it overlaps the transverse resonance. This large (~200 nm in this case) blueshift of the red resonance coupled with the expectation of a relatively smaller shift of the transverse resonance follows the general behavior expected for the two eigenmodes (transverse and longitudinal) of a rod or an ellipsoid as a function of its aspect ratio. However, the dependence of the red-peak resonance on the angle of incidence can not be explained in the model of an isolated rod.

As will be discussed later in the paper, the spectral position of the red peak is indeed related to the longitudinal plasmon resonance of the nanorod, but its behavior is determined by the electromagnetic interaction between the longitudinal resonances of the nanorods in the array. In particular,
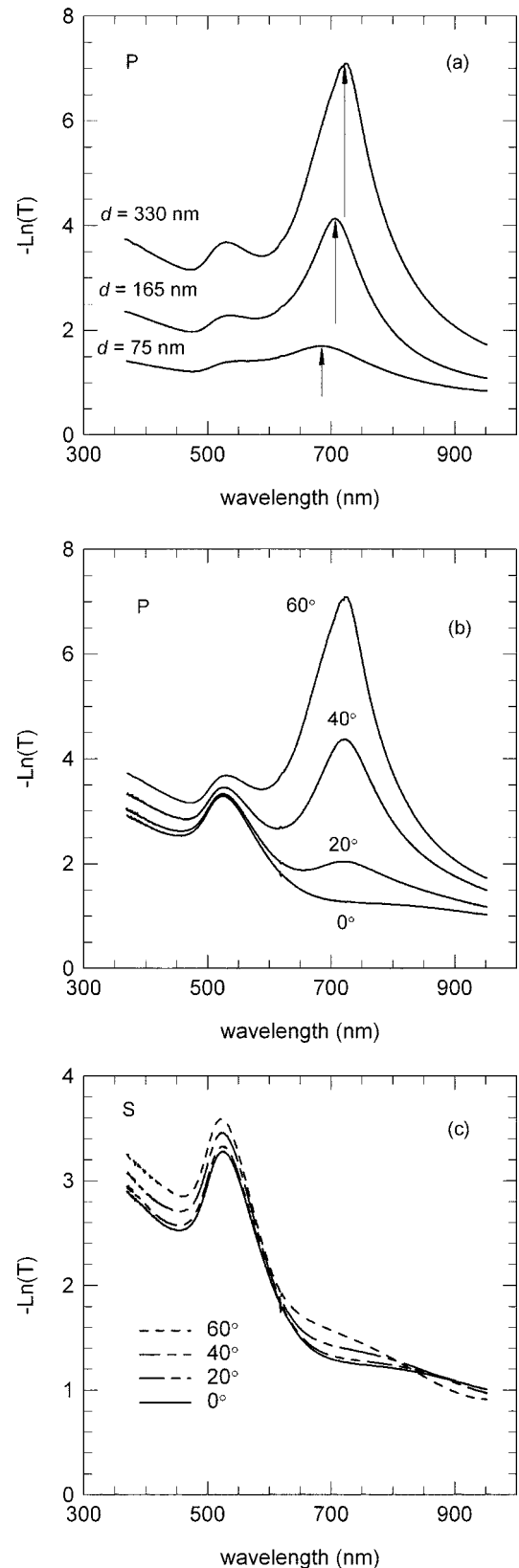
FIG. 3. Transmission data for P-polarized light (a) at 60° angle of incidence and various rod lengths, (b) for 330 nm rods at various angles of incidence, and (c) for S-polarized light for 330 nm rods as a function of angle of incidence.
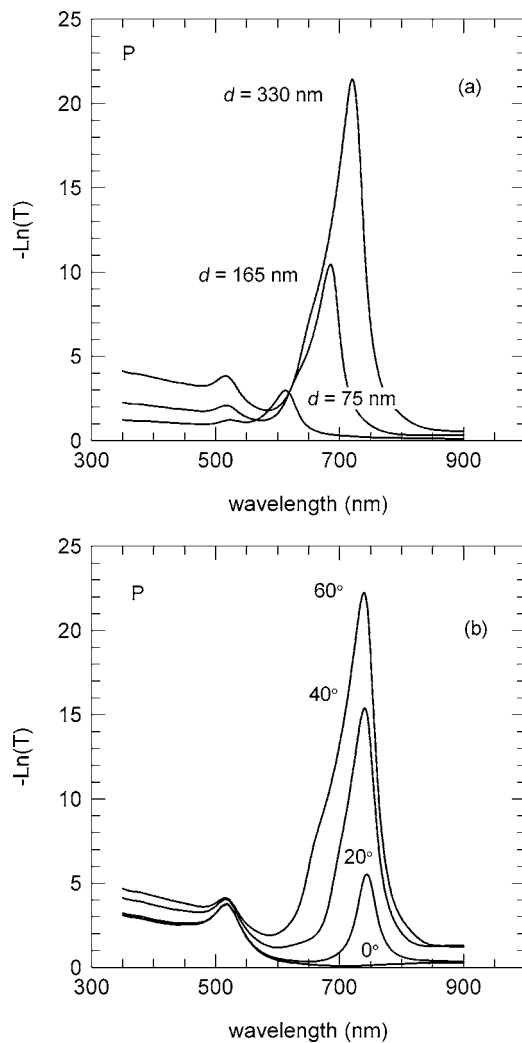
FIG. 4. Calculated transmission data for P-polarized light (a) at 60° angle of incidence and various rod lengths, and (b) for 330 nm rods at various angles of incidence. Using bulk gold data.

FIG. 5. (a) Calculated principal refractive indices for a layer of Au rods of length 75 nm. (b) Effective refractive index n_p for the P-wave within the medium; angle of incidence in air is 60°.

this interaction causes the mode to blueshift, as the spacing between rods is decreased, and experience a small dispersion as the angle of incidence of the incoming light is increased.

We now turn our attention to the modeling of the extinction spectra using the approach outlined in the previous section. In the first instance the optical constants that correspond to bulk materials are used. For this initial comparison we calculate the P-state spectra for the various rod lengths and examine the curves for various angles of incidence for rods of length 330 nm. Moreover, with all other parameters fixed, we use γ_z as a single variable to locate the position of the peaks in the P-state. In this case, $\gamma_z=0.25$, and is an indication that retardation effects between the nanorods in the array may be important and need to be factored into the calculation in a more rigorous way.

Figure 4 allows a direct comparison of the observed [Figs. 3(a) and 3(b)] and calculated curves. It is immediately clear that the positions of the predicted peaks are very close to those observed and that the variation with angle of incidence and rod length is similar. However, whilst the agreement between the two sets of curves is qualitatively good the

quantitative agreement is poor. This is seen in the magnitudes of the values of extinction that differ by a factor of about 4. This is not insignificant and requires explanation. In addition, we point out that the transverse peak shows a definite blueshift with increasing rod aspect ratio, as should be expected.

Before we deal with these quantitative discrepancies it is expedient to explore the reasons that the red peak occurs in the spectral position that it does, according to the anisotropic Maxwell-Garnett model. This is necessary because there is a strong temptation to directly assign the peak to a second localized plasmon resonance associated with the long axis of the rods, as is commonly done where rods are suspended in a liquid and where the interactions between the rods is negligible. To understand the occurrence of this peak we must examine the principal effective refractive indices n_x and n_z, that describe the intrinsic, collective optical properties of the nanorod layer. To illustrate, it is convenient to consider the shortest of the rods (75 nm) where the dispersion of n_x and n_z are shown in Fig. 5(a) together with the corresponding effective refractive index n_p that applies to the P-polarized wave within the medium [Fig. 5(b)], when the incident wave makes an angle of incidence in air of 60°.

With regard to Fig. 5(a), we can identify three regions of interest in the dispersion of the nanorod layer corresponding to three eigenstates of the system. First, the small peak at 525 nm corresponds directly to the optical resonance that is associated with the short axis of the rods. The general shape of the material dispersion in this spectral range is typical of an optical resonance produced by a single damped harmonic oscillator. Accordingly, we might expect the resonance associated with the long axis of the ellipsoid to be revealed by a similar feature at a spectral position where the long wavelength peak is located in Figs. 3 and 4. This is not the case in Figs. 5(a). Instead, the calculations identify the presence of two distinct features that appear at 620 and 1350 nm, where $Im(n_z) \approx Re(n_z)$, and consequently, $Re(\varepsilon_z) \approx 0$. In the spectral range between these wavelengths the nanorod layer permittivity is negative $[Re(\epsilon_z) < 0]$ as for free electron metals and positive in other spectral ranges, where the nanorod layer behaves as a dielectric. It is clear that the experimentally and theoretically observed extinction peak in the red part of the visible spectrum coincides with the point where the real and imaginary parts of n_z are simultaneously equal and small [Fig. 5(a)]. Considering the effective index that applies for the P-wave in the anisotropic medium given by Eq. (8) and shown in Fig. 5(b), in this situation $n_z (\approx 0.2 + i0.2)$ is small compared to $n_x (\approx 2)$ and this results in a large value of $n_P (\approx 2.4 + i2.0)$ and results in the peak that we see experimentally. If we now turn our attention to the resonant feature appearing in the near infrared in Fig. 5(a), we immediately observe the absence of an associated extinction in Fig. 5(b). This is in contrast to the features at 525 and 620 nm that can be excited with a P-wave as shown in Fig. 5(b) and verified experimentally. The reason for the absence of this peak can be appreciated from Eq. (8) where, at the position of the peak, $n_z (\approx 8 + i8)$ is large compared to $n_x (\approx 2)$. This results in a very small value for $Im(n_P)$, and it is therefore not possible to observe this resonance in this experimental configuration.

These observations allow us to conclude as follows on the origin and nature of the longitudinal resonance observed in the optical response of the nanorod array. With respect to the 75 nm rods, the features at 620 and 1350 nm in the calculated dispersion of the nanorod layer [Fig. 5(a)] result from the coherent interaction between the eigenstates corresponding to the longitudinal resonances of the rods in the layer. These hybrid states represent the symmetric and antisymmetric solutions of this interaction. The symmetric state is blueshifted compared to the longitudinal mode of the isolated nanorods (occurring at 850 nm), corresponds to a parallel configuration of the longitudinal transition dipole moments in the rods and is therefore optically active. The mode associated with this state is the red peak observed at 620 nm in the experimental data and modeled spectra. The antisymmetric state reflects the antiparallel arrangement of the dipole moments. This mode is redshifted from the isolated dipole resonance, is not optically active and therefore cannot be observed, in accordance with the anisotropic Maxwell-Garnett theory. The condition $Im(n_z) \approx Re(n_z)$ corresponds to the mode delocalized over the nanorod array. The dependence of the position of this peak on angle of incidence further emphasizes the delocalized character of this state. The
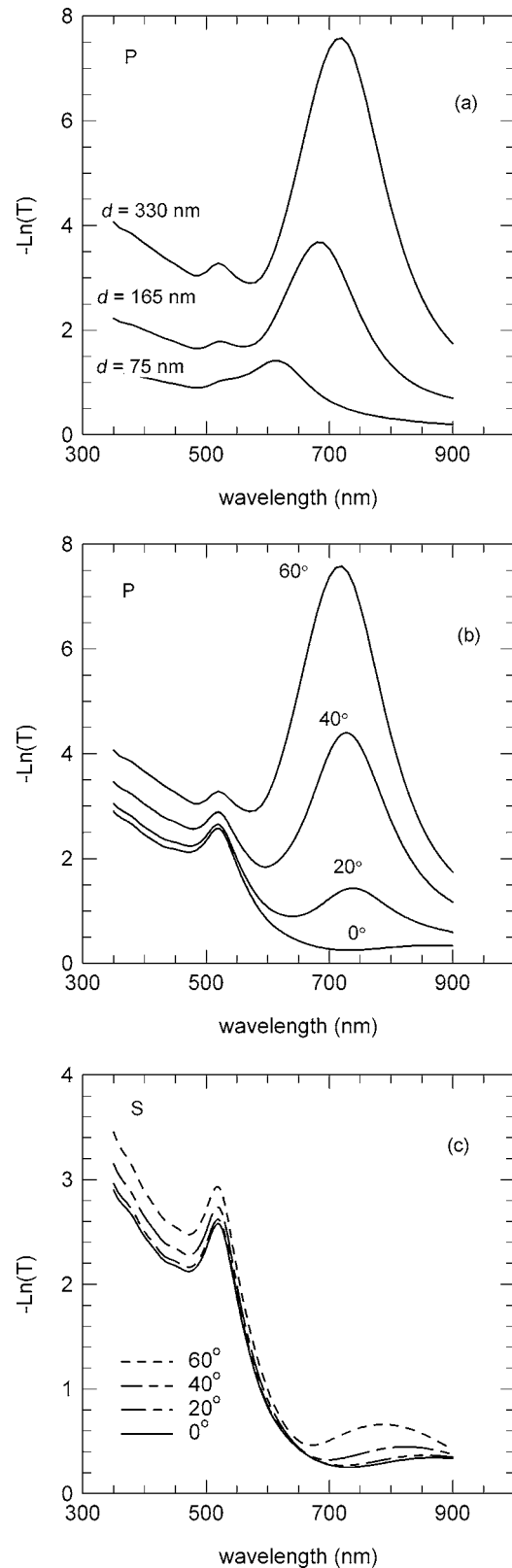
FIG. 6. Calculated transmission data for P-polarized light (a) at 60° angle of incidence and various rod lengths, (b) for 330 nm rods at various angles of incidence, and (c) for S-polarized light for 330 nm rods as a function of angle of incidence using modified gold constants.

detail studies of this delocalization will be presented elsewhere.

EFFECT OF ELECTRON CONFINEMENT

While, in general, the peak positions and dependencies on angle of incidence, polarization state, and rod length are qualitatively described by the Maxwell-Garnett approach, assuming the medium to be anisotropic, there are serious quantitative discrepancies. These discrepancies are not seen in the positions of the peaks but rather in their absolute magnitudes as well as, to some extent, their form and dependencies. Specifically, the calculated curves appear sharper than the measured curves and indicate a material that is much more absorbing than is seen experimentally. The most likely explanation for this lies in the structural integrity of the gold that forms the rods. Unlike thin-film material deposited in ultrahigh vacuum, that closely matches bulk material,[24] the gold here is deposited from solution and may form a very poor physical structure. Moreover, the rods have at least one dimension small compared to the mean free path of electrons in the bulk, and consequently, we might expect to see the influence of electron confinement on their collective behavior at optical frequencies. For simplicity, we assume that the optical properties of gold are described by the responses of the bound and free electrons and that the free electron response is subject to modification where the mean free path between collisions may be restricted physically by particle or grain size. Hence, the dielectric constant of the gold in the rods K_R at angular frequency ω is described by[6]

$$K_R = K_m + \frac{i\omega_P^2 \tau(L-R)}{\omega(\omega\tau+i)(\omega\tau R+iL)}, \quad R \le L, \qquad (9)$$

where $L(=35.7 \text{ nm})$ is the mean free path of the electrons in bulk, R is the effective mean free path, restricted by the effects of structure, $\omega_P(=13.7 \times 10^{15} \text{ Hz})$ is the plasma frequency, and $\tau(=2.53 \times 10^{-14} \text{ s})$ is the relaxation time for the free electrons in gold.

Using Eq. (9) and a value of $R \approx 3$ nm, that is not untypical for small particles of gold,[6] the theoretical curves corresponding to Fig. 3 have been recalculated with the modified optical constants for gold, and these are shown in Fig. 6. Here we have $\gamma_z = 0.3$ to make a small correction to the spectral position of the red peak.

It is important to note that the curves still show all the principal features previously described in relation to peak positions and their dependence on angle of incidence, rod length, and polarization state. Furthermore, they now indicate much lower values of extinction and the peak broadening that is clearly seen in the experimental curves. Moreover, it should be noted that the blueshift of the transverse peak with increasing rod aspect ratio is no longer clear and explains why it is difficult to observe experimentally. In contrast, the blueshifting of the red peak is still quite clear and should be observed.

ANNEALING STUDIES

The application of the anisotropic formulation of the Maxwell-Garnett theory and the dramatic effects that elec-
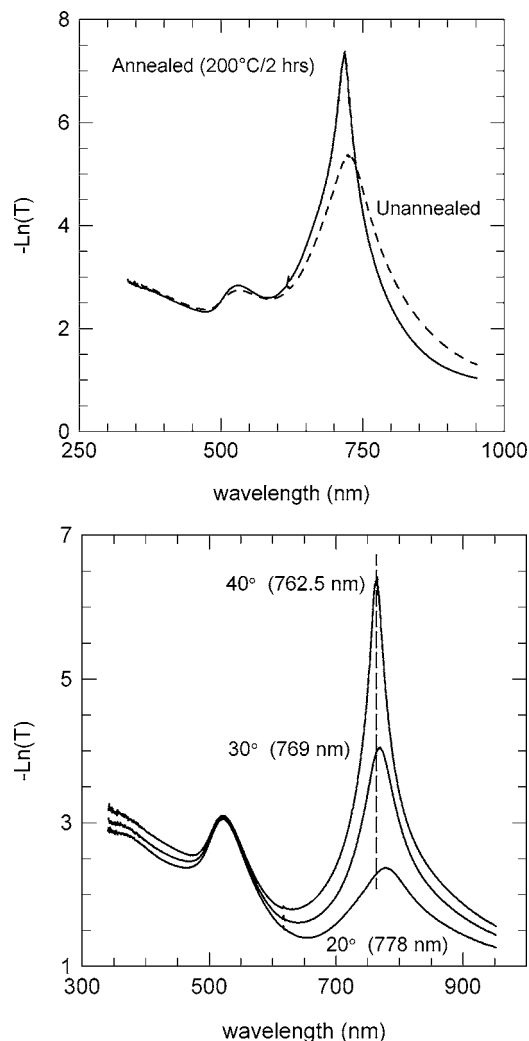
FIG. 7. (a) Experimental transmission data for P-polarized light at 60° angle of incidence for the unannealed and annealed state. Rod length 275 nm. (b) P-state transmission data on an annealed sample showing the blueshift of the red peak with increasing angle.

tron confinement within the gold nanorods has on the optical properties of these assemblies has been clearly demonstrated. However, to gain further evidence for the existence of the size effects and to see if the optical properties may be improved towards expectations based on the intrinsic bulk properties of the materials, we have carried out an annealing study to attempt to induce permanent structural changes within the gold rods. On the basis of the theoretical model outlined above, this should induce observable specific changes in the optical properties. It is expected that annealing may have two effects: it may increase the density of the gold by void removal and hence, reduce rod length and increase the mean free path of the electrons; it may simply increase grain size by crystal growth. It is expected that the impact of these two scenarios will be that the peak heights of extinction will increase and spectral positions may shift, perhaps towards shorter wavelengths if rod length has decreased owing to densification.

A sample having rods of length 270 nm was annealed for 2 h at 200 °C. The results are shown in Fig. 7(a) for an angle

of incidence of 60°. It can be clearly seen that peak height has increased from 5.3 to over 7.4. Moreover, the sharpened peak has clearly shifted slightly towards shorter wavelengths. This is consistent with an increase in density with reduced rod size together with an increase in grain size and thus a relaxation in electron confinement. The results confirm the general conclusions drawn above.

Shown in Fig. 7(b) is the P-state transmission data for a sample having gold rods of length ~400 nm formed in anodized aluminum that was sputter deposited in a partial oxygen atmosphere in an attempt to improve pore ordering. Following this the sample was annealed for 2 h at 200 °C. The blueshifting of the sharpened red peak, as the angle of incidence is increased, is quite clear, as predicted by the MG theory.

CONCLUSION

A series of thin films of gold nanorods within an alumina matrix have been fabricated on top of Au/Ta_2O_5 buffered glass substrates. Optical extinction as a function of rod length, angle of incidence and polarization state have been investigated and analyzed in terms of a theoretical model based on the Maxwell-Garnett theory, adapted for anisotropic media.

For S-polarized incident light, a single peak is seen in extinction that occurs at a wavelength of ~525 nm and is associated with the transverse plasmon resonance that corresponds to the short axis of the rods. The peak position is not strongly dependent on rod length or angle of incidence.

Optical properties of the nanorod arrays studied with P-polarized probe light indicate that a second redshifted resonance is strongly dependent on rodlength and angle of incidence, and is related to the longitudinal resonances of the nanorods. A quantitative analysis of the experimental data, using the anisotropic Maxwell-Garnett theory, indicates that for given nanorod array parameters, the strong electromagnetic interaction between localized longitudinal resonances within individual nanorod leads to a splitting of this mode and the formation of coupled modes of the array. The observed redshifted peak corresponds to the shorter wavelength shifted parallel coupled plasmon resonance. It is shown that its counterpart, the longer wavelength shifted antiparallel coupled resonance, is not optically active.

The quantitative data presented here when compared to the theoretical model also suggest a strong dependency of the observations on the modified optical properties of the gold nanorods due to confinement of conduction electrons as a consequence of poor grain structure. Taking this into account allows very good agreement between observation and theory. The above observations are supported by annealing studies where the physical structure of the gold within the nanorods is modified to produce more bulk-like properties that result in predictable changes of the anisotropic optical properties of the nanorod arrays.

[1] S. Link and M. A. El-Sayed, J. Phys. Chem. B **103**, 8410 (1999).

[2] N. Fang, H. Lee, C. Sun, and X. Zhang, Science **308**, 534 (2005).

[3] R. Zong, J. Zhou, B. Li, M. Fu, S. Shi, and L. Li, J. Chem. Phys. **123**, 094710 (2005).

[4] S. Melle, J. L. Menéndez, G. Armelles, D. Navas, M. Vázquez, K. Nielsch, R. B. Wehrspohn, and U. Gösele, Appl. Phys. Lett. **83**, 4547 (2003).

[5] M. Darques, A. Encinas, L. Vila, and L. Piraux, J. Phys. D **37**, 1411 (2004).

[6] P. H. Lissberger and R. G. Nelson, Thin Solid Films **21**, 159 (1974).

[7] P. H. Lissberger and P. W. Saunders, Thin Solid Films **34**, 323 (1976).

[8] D. Felbacq and G. Bouchitté, New J. Phys. **7**, 159 (2005).

[9] A. N. Grigorenko, A. K. Geim, H. F. Gleeson, Y. Zhang, A. A. Firsov, I. Y. Khrushchev, and J. Petrovic, Nature (London) **438**, 335 (2005).

[10] V. M. Shalaev, W. S. Cai, U. K. Chettiar, H. k. Yuan, A. K. Sarychev, V. P. Drachev, and A. V. Kildishev, Opt. Lett. **30**, 3356 (2005).

[11] G. Mie, Ann. Phys. **25**, 377 (1908).

[12] R. Gans, Ann. Phys. **4**, 270 (1915).

[13] J. C. Maxwell-Garnett, Philos. Trans. R. Soc. London **203**, 385 (1904); , Philos. Trans. R. Soc. London **205**, 237 (1906).

[14] C. Douglas, P. Evans, and R. J. Pollard, Technical Proceedings of the 2005 NSTI Nanotechnology Conference and Trade Show, 2005, Vol. 2, 385.

[15] M. J. Liew, S. Roy, and K. Scott, Green Chem. **5**, 376 (2003).

[16] E. M. Purcell and C. R. Pennypacker, Astrophys. J. **186**, 705 (1973).

[17] G. L. Hornyak, C. J. Patrissi, and C. R. Martin, J. Phys. Chem. B **101**, 1548 (1997).

[18] F. J. Garcia-Vidal, J. M. Pitarke, and J. B. Pendry, Phys. Rev. Lett. **78**, 4289 (1997).

[19] C. F. Bohren and D. R. Huffman, *Absorption and Scattering of Light by Small Particles*, John Wiley & Sons (1998).

[20] S. F. Nee, Appl. Opt. **27**, 2819 (1988).

[21] P. H. Lissberger, Rep. Prog. Phys. **33**, 197 (1970).

[22] A. N. Lagarkov and A. K. Sarychev, Phys. Rev. B **53**, 6318 (1996).

[23] C. Sönnichsen, T. Franzl, T. Wilk, G. von Plessen, J. Feldmann, O. Wilson, and P. Mulvaney, Phys. Rev. Lett. **88**, 077402 (2002).

[24] P. H. Lissberger, I. W. Salter, M. Fitzpatrick, and P. L. Taylor, J. Phys. E **10**, 635 (1977).